XLVI CILAMCE
VITÓRIA - ES - BRAZIL - 2025
XLVI IBERO-LATIN AMERICAN CONGRESS ON COMPUTATIONAL METHODS IN ENGENEERING

CFD Analysis of Urban Airflow in a Mining-Influenced Neighborhood Considering Real Topography Data Relevance

Eduardo de S. P. Miranda[1], Renata D. Corrêa[2], Bruna L. V. Maia[3], Bruno Furieri [2], Taciana T. de Albuquerque[3]

[1] Dept. of Mechanical Engineering, University of Minas Gerais
Av. Pres. Antônio Carlos, 6627, 31270-901, Minas Gerais, Brazil
eduardopescada@gmail.com
[2] Dept. of Environmental Engineering Federal University of Espírito Santo
Av. Fernando Ferrari 514, 29075-910, Espírito Santo, Brazil
redrummondc@outlook.com, bruno.furieri@gmail.com
[3]Dept. Of Sanital and Ambial Engineering, Federal University of Minas Gerais
Av. Pres. Antônio Carlos, 6627, 31270-901, Minas Gerais, Brazil
brunalimaveras@gmail.com, tacianatoledo26@gmail.com

Abstract. Urban areas located near ore management or mining sites may be affected by air pollution caused by the emission of particulate matter resulting from activities associated with the mineral production chain. This study evaluates, through Computational Fluid Dynamics (CFD), the effects of the terrain in wind flow over blocks in a city of Minas Gerais, Brazil, using real topography and constructions present in the area. The focus was visualization of velocity gradients in the wind stream and turbulent patterns that may represent areas of deposition, recirculation and reemission of particulate matter. It was found that the terrain plays a relevant and indispensable role in real world analysis.

Keywords: CFD, particulate matter emission, urban areas, real topography.

1 Introduction

In certain urban areas, air pollution may result from the emission of particulate matter originating from nearby mining and mineral processing activities. Besides the deposition of dust on roads, plants and houses everywhere along the wind stream, suspended particulate matter has negative effects on the population's health, from aggravating to being the root cause of cardiovascular and respiratory diseases, as Goudie [1] presents. Accordingly, the present study aims to evaluate the airflow through the streets and between residential blocks located in a neighborhood within the urban area of a municipality in the state of Minas Gerais, situated near mining activities, using computational fluid dynamics (CFD). For this purpose, the software Ansys Fluent was employed to carry out the computational simulations, in which the actual topography of the terrain related to the studied case was considered. Recent works, Zeynab Kaseb [2] and Blocken [3], in particulate matter carried by wind uses simplified geometry of the terrain to model the basis of the air flow in urban regions. In contrast, the present analysis uses the official terrain scan made available by the city hall which excludes buildings and vegetation, but considers the detailed topography. Analyzing one of the eighth cardinal wind directions, North-South, it is possible to identify areas with low and high wind velocities, in which may occur deposition and emission of particulate matter, as Shao and Lu [4] shown. Furthermore, the integrated use of these tools and datasets enables a quantitative assessment of the performance of existing strategies in controlling particulate matter emissions.

2 Methodology

The terrain topology and images were granted by the city hall in high resolution. The software QGis 3.34 was adopted along with the complements 'Raster' and 'Google Hybrid view'. Terrain data was extracted as a 3D file of the desired region and employed in the modeling software ANSYS SpaceClaim, also, the above view granted by the city hall was aligned over the topology terrain. By this overlap, all relevant buildings present in the area were drawn as a surface over the above view, then lowered until its center intersected the terrain (Figure 1). After that, through Google Street view the height of each one was estimated using an expected height of 3 meter per floor and 7,5 meters for industrial related constructions. the contextual information about each building was considered as well, for example, the presence of a truck parked under it, as shown in figure 2.

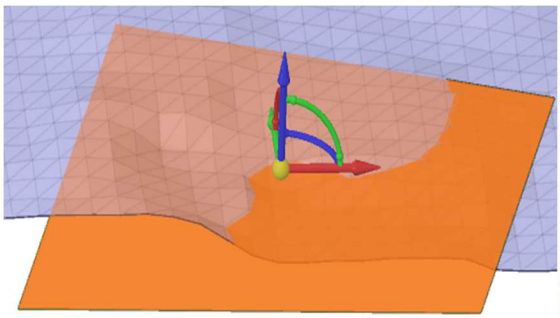


Figure 1 – Geometric center of the building surface representation intersecting the terrain surface.

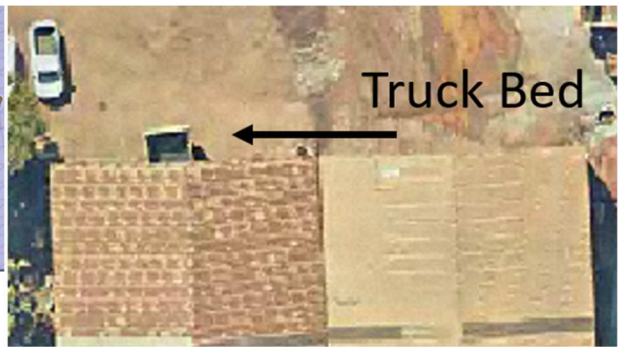
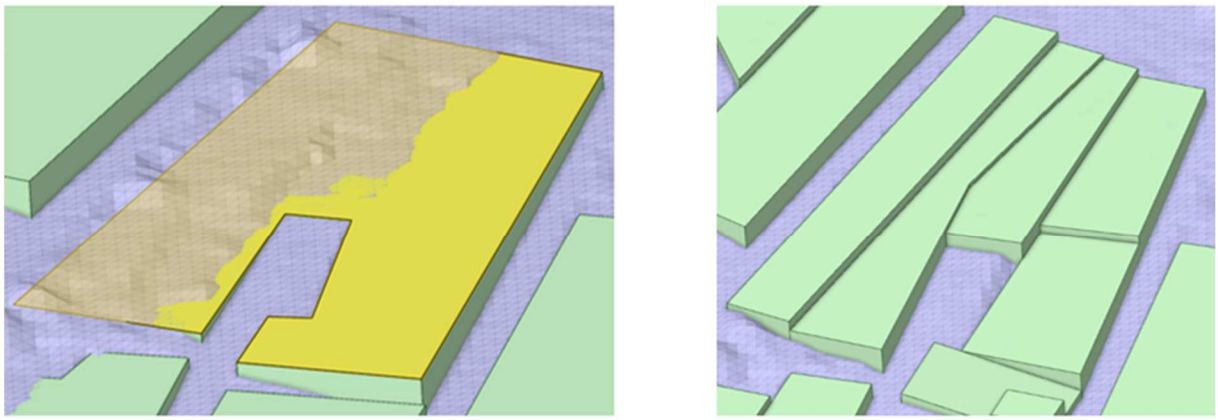


Figure 2 - Truck bed underneath industrial construction

As the majority of building agglomerations present in the studied are in rough terrain, it was impossible to consider each of them as a unique solid. Therefore, due to the terrain inclination, each block was segmented into multiple sections where necessary, as depicted in Figure 3. As a final step, every solid was stretched until it fully intersected the terrain to guarantee no gaps. Furthermore, Silva [5] recommends a uniform region for the outlet boundary to minimize potential numerical instability. In line with this recommendation and supported by the guidelines of Versteeg & Malalasekera [6], the original neighborhood domain was elongated 80 meters in each direction to guarantee a developed wind flow over the interested area of study. Figure 4 displays the surface domain and its spatial elongation.



(a) (b)

Figure 3 - Example of a building block segmentation: (a) non-segmented block; (b) segmented block.

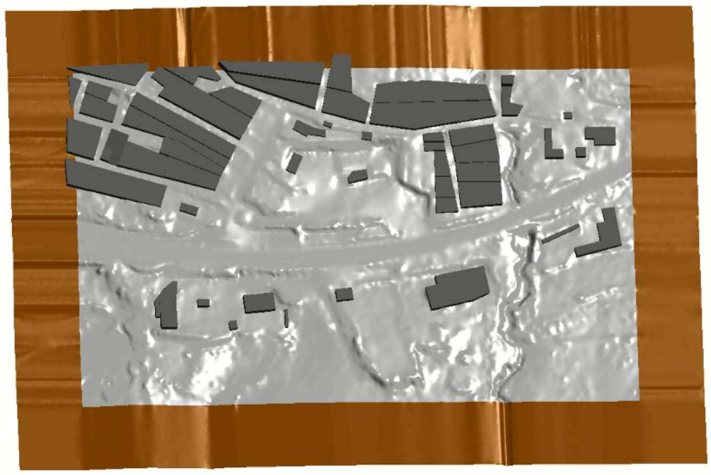


Figure 4 - Surface domain in light gray, buildings in dark gray and elongations in brown.

The simulations were conducted using ANSYS Fluent software and the turbulent model K-Epsilon RNG with Standard Wall Functions. It is capable of solving the Navier-Stokes equations, given by:

- The continuity equation

$$\frac{\partial \rho}{\partial t} + \nabla \cdot (\rho v) = 0 \tag{1}$$

- The momentum equations

$$\frac{\partial}{\partial t}(\rho v) + \nabla \cdot (\rho v \cdot v) = -\nabla p + \nabla \cdot (\underline{\tau}) + \rho g + F \tag{2}$$

Where t is time, and v is the velocity field, ρ is density, $\underline{\tau}$ is the stress tensor, g is gravity, F is external forces actuating in the domain and p is pressure.

The turbulence model used was the RNG K-ϵ model. It solves two transport equations, one for the turbulent kinetic energy k and one for the turbulent

- K - equation

$$\frac{\partial}{\partial t}(\rho k) + \frac{\partial}{\partial x_i}(\rho k u_i) = \frac{\partial}{\partial x_j}\left[\alpha_k \mu_{eff} \frac{\partial k}{\partial x_j}\right] + G_k + G_b - \rho\varepsilon - Y_M + S_k \tag{3}$$

- ε - equation

$$\frac{\partial}{\partial t}(\rho \varepsilon) + \frac{\partial}{\partial x_i}(\rho \varepsilon u_i) = \frac{\partial}{\partial x_j}\left[\alpha_\varepsilon \mu_{eff} \frac{\partial \varepsilon}{\partial x_j}\right] + C_{1\varepsilon}\frac{\varepsilon}{k}(G_k + C_{3\varepsilon}G_b) - C_{2\varepsilon}\rho\frac{\varepsilon^2}{k} - R_\varepsilon + S_\varepsilon \tag{4}$$

In these equations, G_k represents the generation of turbulence kinetic energy due to the mean velocity gradients, G_b is the generation of turbulence kinetic energy due to buoyancy, Y_M represents the contribution of the fluctuating dilatation in compressible turbulence to the overall dissipation rate, The quantities α_k and α_ε are the inverse effective Prandtl numbers for k and ε, respectively.

It was decided to not present the equations that calculate these variables due to the extension of its mathematical formulations. Nevertheless, detailed explanation and formulations can be found in ANSYS [7].

The mesh was generated in ANSYS Mesh with Prismatic boundary layers. It was generated with 25 layers, an initial height of 0.02 meters, a layer growth rate of 1.2, and an overall thickness of 9.44 meters. The height of the first layer was defined after small scale tests were conducted with part of the original domain, aiming to reach

y+ values over the surface between 30 and 300 [7]. The final mesh reached the desired y+ range. Also, the mesh was constructed with tetrahedron cells. The average elementary quality was 0.347 and the average skewness was 0.261. All other parameters were automatically determined by the default element size of 20 meters, resulting in 2,039,954 nodes and 4,568,826 elements. Mesh details are shown in Figure 5.

The simulations were conducted in a steady-state regime using Fluent software. A velocity inlet boundary was set in the South face with a uniform velocity profile of 5 m/s and a pressure outlet boundary was set in the North face with atmospheric pressure. The residual monitor and the average velocity in 9 different lines, near buildings or in open fields, as displayed in Figure 6, were used to evaluate the simulation conversion.

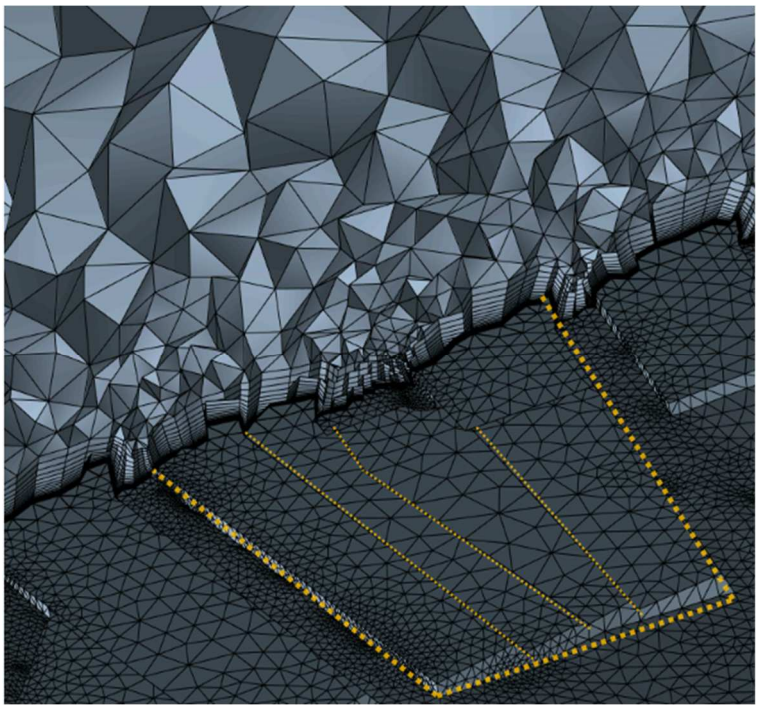


Figure 5 - Prismatic layer of the block presented in Figure 3.

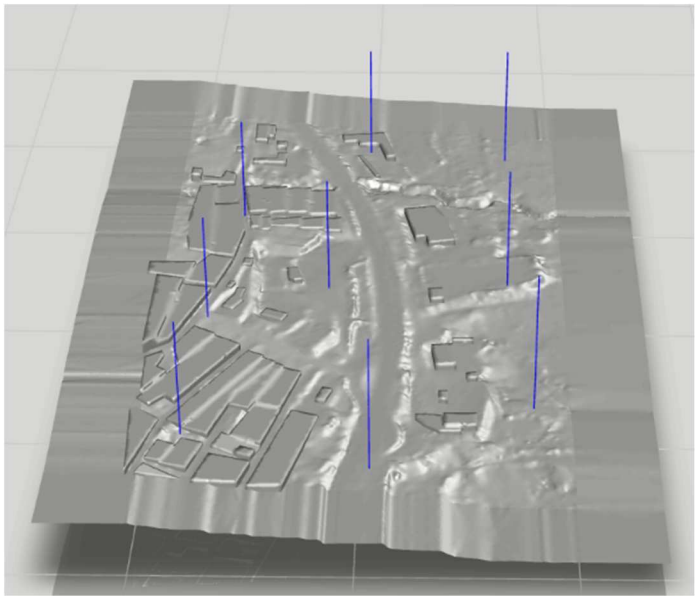


Figure 6 – Geometric lines adopted to simulation monitoring.

Through a meteorological station located near the neighborhood, it was possible to evaluate that the wind direction South-North is one of the principal directions throughout the year according to INMET [8]. Thus, considering the real word relevance, this direction was chosen to be simulated for this paper. About the velocity wind speedy, weather station data indicate that the average annual wind speed is 2 m/s and the average maximum wind gust reaches 14 m/s, with gusts around 5 m/s being more frequently observed. Therefore, considering the type of particulate matter emitted by mining and mineral processing activities — which is known to include heavier particles that Silvester [9] point out that are not easily lifted — and the low overall frequency of higher wind gusts such as 14 m/s, a wind speed of 5 m/s was adopted for the studied domain.

3 Results

Particulate matter, after being airborne, deposits whenever the velocity of the wind stream that carries it reduces, as discussed by Jeong and Han [10]. Thereby, the visualization of low-speed air flow indicates areas of dust deposition over the neighborhood, which can be inferred from streamline distribution. Figures 6 and 7 are examples of low speed vortexes formed after buildings and are indicators of potential areas with dust accumulation.

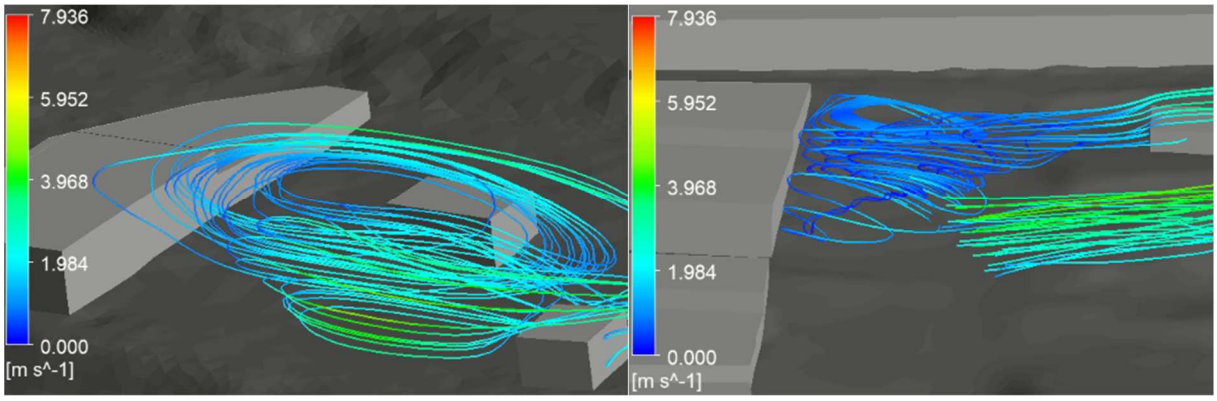


Figure 7 - Velocity streamlines downstream of building blocks.

The terrain also influences how the wind flow behaves behind structures. In Figure 8(a), the pink circle indicates where it is possible to notice the speed reduction caused by the flow in the area between them. Similarly, Figure 8(b) shows a low speed region forming a pocket between the building and the terrain, which inhibits the deceleration of the air flowing over the building (orange arrow). Considering the side flow, demonstrated by the pink arrow, would have already deposited the particulate matter it was carrying due to its already low velocity, this phenomenon might reduce the dust settling of the flow over the structure without promoting any additional dust deposition.

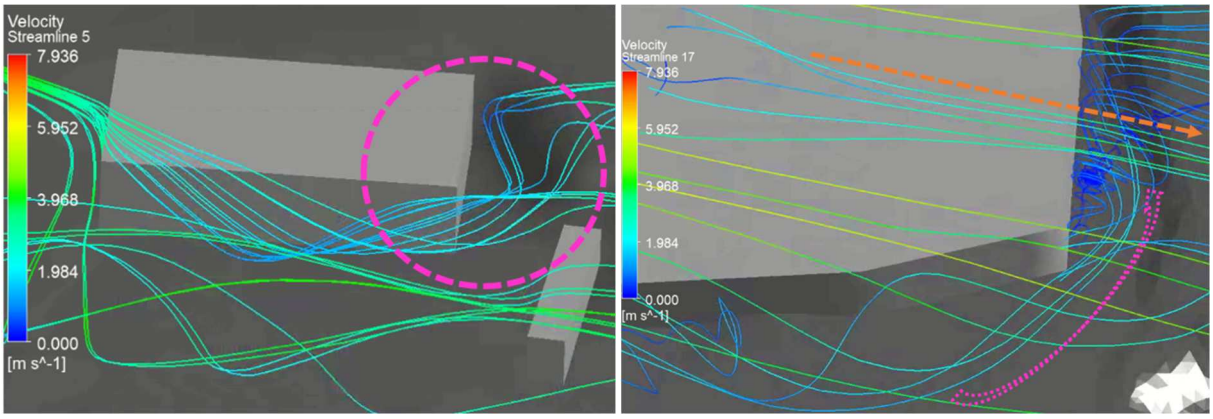


Figure 8 - Velocity streamlines near building blocks: (a); deceleration caused by terrain (pink circle) and (b) pocket of low-speed turbulence and undisturbed wind current (orange arrow).

As a final point, the terrain affects the wind speed significantly, resulting in sharp gradients of velocity and, consequently, regions of great dispersion and deposition of dust. This phenomenon is displayed by Figure 10, where the topology causes wind stream acceleration and deceleration, which, notably, corresponds to one of the areas of highest wind speeds.

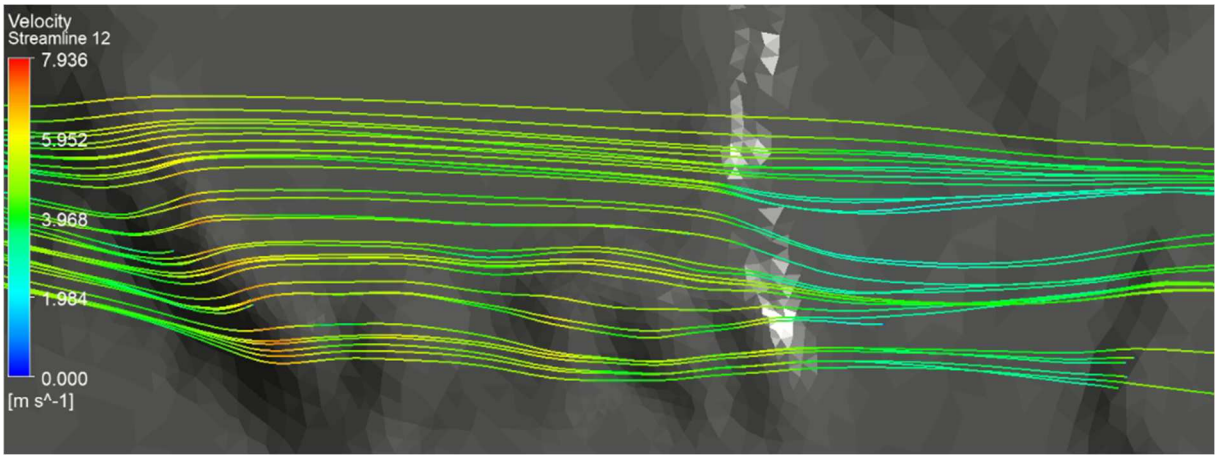


Figure 9 – Velocity streamlines representing the flow immediately above tortuous terrain

4 Conclusions

The present work intended to demonstrate the relevance of the topography in real world CFD analysis. This objective was reached, as the terrain clearly interfered in the wind speed and flow over the city neighborhood, promoting locations where deposition and emission of particulate matter could be increased or reduced. The variation of air velocity up to 7.936 m/s indicates considerable emissions of this pollutant and potential harmful health impacts over the regional population.

Moreover, the methodology and results supports the identification of optimal technologies and spatial deployment strategies for future interventions aimed at achieving effective dust pollution reduction. Vegetation already present is aimed to be analyzed in future studies along with the other 7 wind directions and proposals of new Green Barriers.

Acknowledgements. This study was financed by PIBIC (Programa Institucional de Bolsas de Iniciação Científica) CNPq and FAPEMIG and the Project n. 230.72.260.580/2023-49. We also thank the Coordenação de Aperfeiçoamento de Pessoal de Nível Superior (CAPES) for providing free access to scientific journals, which was essential for the development of this work. Special thanks are extended to the GPAMA (Grupo de Pesquisa em Poluição do Ar e Meteorologia Aplicada) research group for their technical support and collaboration throughout this study.

Authorship statement. The authors hereby confirm that they are the sole liable persons responsible for the authorship of this work, and that all material that has been herein included as part of the present paper is either the property (and authorship) of the authors, or has the permission of the owners to be included here.

References

[1] Andrew S. Goudie, “Desert dust and human health disorders”. *Environment International,* 2014

[2] Zeynab Kaseb et al. “A framework for pedestrian-level wind conditions improvement in urban areas: CFD simulation and optimization”, *Building and Environment*, 2020

[3] B. Blocken, W.D. Janssen, T. van Hooff, "CFD simulation for pedestrian wind comfort and wind safety in urban areas: General decision framework and case study for the Eindhoven University campus", *Environmental Modelling & Software*, 2012

[4] Yaping Shao, Hua Lu, "A simple expression for wind erosion threshold friction velocity", *JOURNAL OF GEOPHYSICAL RESEARCH*, 2000

[5] Silva, C. A. M. Computational study of atmospheric flows over Perdigão: terrain resolution and domain size, 2018

[6] Versteeg, H., & Malalasekera, W. An Introduction to Computational Fluid Dynamics: The Finite Volume Method: Vol. M (2nd ed.). 2007

[7] ANSYS INC. *ANSYS Fluent Theory Guide: Chapter 4 — Near-Wall Treatment*. Canonsburg, PA: ANSYS Inc., 2024

[8] INMET, https://bdmep.inmet.gov.br, 2023

[9] S.A. Silvester, I.S. Lowndes, D.M. Hargreaves, "A computational study of particulate emissions from an open pit quarry under neutral atmospheric conditions", *Atmospheric Environment*, 2009

[10] Jeong, N.-R.; Han, S.-W.;Kim, J.-H, "Evaluation of VegetationConfiguration Models for Managing Particulate Matter along the Urban Street Environment", *Forests*, 2022